Mammalian formin Fhod3 plays an essential role in cardiogenesis by organizing myofibrillogenesis

Meikun Kan-o[1,*], Ryu Takeya[1,*], Takaya Abe[2], Naoyuki Kitajima[3], Motohiro Nishida[3], Ryuji Tominaga[4], Hitoshi Kurose[3] and Hideki Sumimoto[1,‡]

[1]Department of Biochemistry, Kyushu University Graduate School of Medical Sciences, 3-1-1 Maidashi, Higashi-ku, Fukuoka 812-8582, Japan
[2]Laboratory for Animal Resources and Genetic Engineering, RIKEN Center for Developmental Biology, Kobe, Hyogo 650-0047, Japan
[3]Department of Pharmacology and Toxicology, Kyushu University Graduate School of Pharmaceutical Sciences, 3-1-1 Maidashi, Higashi-ku, Fukuoka 812-8582, Japan
[4]Department of Cardiovascular Surgery, Kyushu University Graduate School of Medical Sciences, 3-1-1 Maidashi, Higashi-ku, Fukuoka 812-8582, Japan

*These authors contributed equally to this work
‡Author for correspondence (hsumi@med.kyushu-u.ac.jp)

Biology Open 1, 889–896
doi: 10.1242/bio.20121370
Received 21st March 2012
Accepted 18th June 2012

Summary

Heart development requires organized integration of actin filaments into the sarcomere, the contractile unit of myofibrils, although it remains largely unknown how actin filaments are assembled during myofibrillogenesis. Here we show that Fhod3, a member of the formin family of proteins that play pivotal roles in actin filament assembly, is essential for myofibrillogenesis at an early stage of heart development. *Fhod3*$^{-/-}$ mice appear normal up to embryonic day (E) 8.5, when the developing heart, composed of premyofibrils, initiates spontaneous contraction. However, these premyofibrils fail to mature and myocardial development does not continue, leading to embryonic lethality by E11.5. Transgenic expression of wild-type Fhod3 in the heart restores myofibril maturation and cardiomyogenesis, which allow *Fhod3*$^{-/-}$ embryos to develop further. Moreover, cardiomyopathic changes with immature myofibrils are caused in mice overexpressing a mutant Fhod3, defective in binding to actin. These findings indicate that actin dynamics, regulated by Fhod3, participate in sarcomere organization during myofibrillogenesis and thus play a crucial role in heart development.

Key words: Actin, Fhod3, Formin, Myofibrillogenesis, Sarcomere

Introduction

The heart is the first organ to form and function during embryogenesis, and assures biological activities throughout the life by its contractile activity. Sufficient contraction of the developing heart requires maturation of myofibrils, composed of repeating units known as sarcomeres, where arrays of actin (thin) and myosin (thick) filaments comprise the contractile apparatus (Clark et al., 2002). In the sarcomere, barbed ends of actin filaments are anchored in the Z-line, and their pointed ends extend into the middle of the sarcomere. The initiation of the heartbeat occurs before sarcomere maturation (and thus before myofibril maturation), and is followed by myocardial development with trabeculation (formation of finger-like projections of the myocardium into the ventricular lumen) and by chamber formation, which begins with looping of the heart tube (Moorman and Christoffels, 2003; Taber, 1998). The molecular mechanisms by which the sarcomere is organized during cardiogenesis remain poorly understood.

During sarcomere organization in the striated muscle (*i.e.*, the skeletal and cardiac muscles), actin cytoskeleton undergoes dynamic rearrangement to form mature actin filaments with uniform length and polarity (Gregorio and Antin, 2000; Littlefield and Fowler, 2008; Ono, 2010; Sanger et al., 2005). At the beginning of sarcomere organization, the I-Z-I complex (a.k.a. the Z-body) emerges in premyofibrils as a precursor of the Z-line: the complex contains filamentous actin and a cluster of Z-line proteins such as α-actinin. Subsequent alignment of the precursors leads to formation of a striated pattern of the Z-line; and unanchored (pointed) ends of actin filaments become aligned with uniform length at the final step in sarcomere organization for maturation of myofibrils (Gregorio and Antin, 2000). Several actin-associating proteins have recently been proposed as key regulator of actin dynamics during myofibrillogenesis. Nebulin, a giant actin-binding protein in the sarcomere, participates in actin filament formation in the skeletal muscle (Takano et al., 2010), whereas leiomodin, a protein related to the pointed-end capping protein tropomodulin (Tmod), serves as an actin filament nucleator in cardiomyocytes (Chereau et al., 2008). Another likely candidate for a key regulator in the cardiac muscle is Fhod3 (a.k.a. Fhos2), a member of formin family proteins (Kanaya et al., 2005). Formins are characterized by the presence of the FH1 (formin homology 1) and FH2 domains: the latter one possesses actin nucleation and polymerization activities, which are accelerated by FH1-mediated recruitment of the profilin-actin dimer (Paul and Pollard, 2009). Through cooperation by the two domains, formins direct formation of straight actin filaments

(Goode and Eck, 2007; Pollard, 2007), thereby regulating diverse cytoskeletal reorganization during development (Chesarone et al., 2010; Liu et al., 2010). Fhod3, as well as Dishevelled-associated activator of morphogenesis 1 (Daam1), is a major formin in the heart (Kanaya et al., 2005; Li et al., 2011), although its truncated form is expressed in the brain and kidney (Kanaya et al., 2005). RNA interference-mediated depletion of Fhod3 in cultured cardiomyocytes disrupts sarcomere organization (Iskratsch et al., 2010; Taniguchi et al., 2009), suggesting a role of Fhod3-regulated actin dynamics. However, the role of Fhod3 in development has remained to be elucidated.

Here we show that knock out of the *Fhod3* gene in mice confers lethality by embryonic day (E) 11.5 with a massive pericardial effusion. Embryonic development of *Fhod3*$^{-/-}$ mice appears normal up to E8.5. Although the developing heart tube consisting of a thin layer of the myocardium initiates spontaneous contraction and rightward looping, subsequent chamber formation and myocardial development with trabeculation are aborted in *Fhod3*$^{-/-}$ embryos. The embryonic lethality is probably due to cardiac defects, since transgenic expression of Fhod3 in the heart allows embryos to develop until before birth. In the absence of Fhod3, myofibrils in the developing heart remain premature, *i.e.*, they are thin and sparsely distributed with irregularly spaced dots of α-actinin. Thus Fhod3 appears to play a crucial role in sarcomere (and myofibril) maturation during myocardial development.

Materials and Methods

Generation of *Fhod3* knockout mice and transgenic mice overexpressing Fhod3

The *Fhod3* knockout mouse (Acc. No. CDB0598K: http://www.cdb.riken.jp/arg/mutant%20mice%20list.html) was generated according to the protocols as described (http://www.cdb.riken.jp/arg/Methods.html). In brief, the 5′ homologous arms (7.5 kb) was isolated by the Red/ET recombination cloning system (Gene Bridges GmbH) and the 3′ arms (3.5 kb) was amplified by PCR using a BAC clone RPCI23-304D8 and subcloned into the DT-ApA/LacZ/Neo cassette (RIKEN CDB: http://www.cdb.riken.jp/arg/cassette.html) to generate the targeting vector. The linearized targeting vector was electroporated into TT2 embryonic stem cells (Yagi et al., 1993), and G418-resistant clones were screened by PCR and confirmed by Southern blot analysis to identify ones with correct homologous recombination. The PCR products from the wild-type and recombinant alleles were 655 bp and 862 bp in length, respectively. Chimeric mice were generated with the recombinant embryonic stem cell clones and mated with C57BL/6 females to generate heterozygous animals (*Fhod3*$^{+/-}$), which were maintained on the C57BL/6 genetic background. Two mutant strains generated from two independent recombinant embryonic stem cell clones were analyzed. No phenotypic differences between the two strains were observed.

Transgenic mice expressing wild-type Fhod3 (GenBank/EMBL/DDBJ accession NO. AB078608) (Kanaya et al., 2005) under the control of the α-myosin heavy chain promoter, a generous gift from Dr. Jeffery Robbins (Cincinnati Children's Hospital Medical Center) (Gulick et al., 1991), were generated on a C57BL/6 background, as previously described (Kan-o et al., 2012); expression level of exogenous Fhod3 in the transgenic mice was ten-fold more than that of endogenous Fhod3. Transgenic mice expressing a mutant Fhod3 carrying the I1127A substitution (Taniguchi et al., 2009) under the control of the α-myosin heavy chain promoter were also generated on a C57BL/6 background. Expression level of the mutant Fhod3 in the transgenic mice was ten-fold more than that of endogenous (wild-type) Fhod3 (supplementary material Fig. S4).

All mice were kept in a specific pathogen-free animal facility at Kyushu University. All procedures using mice were performed in strict accordance with the guidelines for Proper Conduct of Animal Experiments (Science Council of Japan). The experimental protocol was approved by the Animal Care and Use Committee of Kyushu University (Permit Number: A22-005-1). All efforts were made to minimize the number of animals used and their suffering.

LacZ staining

LacZ staining of heterozygous *Fhod3*$^{+/-}$ embryos was performed as described by Shima et al. (Shima et al., 2005). Briefly, timed pregnant mice were sacrificed via cervical dislocation and embryos were dissected from the uterus. Embryos were fixed at 4℃ by immersion in phosphate-buffered saline (PBS: 137 mM NaCl, 2.68 mM KCl, 8.1 mM Na_2HPO_4, and 1.47 mM KH_2PO_4, pH 7.4) containing 1% formaldehyde, 0.2% glutaraldehyde, 0.02% Nonidet P-40, and 1 mM $MgCl_2$. The whole body of embryos was incubated overnight at 37℃ in PBS containing 1 mg/ml X-gal, 5 mM $K_3Fe(CN)_6$, 5 mM $K_4Fe(CN)_6$, and 2 mM $MgCl_2$. For detailed observation of cardiac looping, the head and tail were excised.

Histological analysis

Timed pregnant mice were sacrificed via cervical dislocation and embryos were dissected from the uterus. Dissected embryos were fixed by immersion in a solution containing 3.7% formaldehyde in PBS at 4℃. In the case of embryos at E17.5, the heart was removed from mice under hypothermal anesthesia (Kulandavelu et al., 2006) and then fixed. Fixed embryos or hearts were dehydrated in ethanol, embedded in paraffin, sectioned, and stained with hematoxylin and eosin.

Immunofluorescence staining

Timed pregnant mice were sacrificed via cervical dislocation and the uterus was removed. Embryos at E8.5–13.5 were dissected in cold PBS, and the whole body was fixed by immersion in 3.7% formaldehyde for 6 h (E8.5) or for 12 h (E9.5–13.5) at 4℃. E17.5 embryos were anesthetized by hypothermia, whereas 8-day-old neonates were anesthetized by sevoflurane inhalation. They were subjected to perfusion fixation as follows: after clamping of the ascending aorta and clipping of the right atrium, 1 ml of PEM buffer (1 mM EGTA, 1 mM $MgCl_2$, and 100 mM PIPES, pH 6.9) containing 20 mM KCl was administrated from the left ventricle using a pulled capillary tube, followed by perfusion of 3 ml of 3.7% formaldehyde. The fixed hearts were removed from the deceased mice, cut into small pieces, and immersed for 90 min at 4℃ in the same fixative for post-fixation. The fixed whole embryo or heart was washed in PBS, subjected to osmotic dehydration overnight at 4℃ in 30% sucrose, and embedded in OCT compound (Sakura Finetek). The blocks were frozen and cut into 5 µm sections using a cryostat (HM550; Thermo Scientific). Then sections were washed with PBS containing 0.1% Triton X-100, and blocked with a blocking buffer (PBS containing 3% bovine serum albumin and 2% goat serum) for 2 h at room temperature. Sections were labeled overnight at 4℃ with primary antibodies diluted in the blocking buffer containing 0.1% Triton X-100, washed in PBS containing 0.1% Triton X-100, and then labeled for 1 h at 37℃ with a fluorescein-conjugated secondary antibody mixture in the same buffer containing Alexa-594-phalloidine (Invitrogen) for F-actin staining. Images were taken with an LSM510 confocal scanning laser microscope (Carl Zeiss MicroImaging).

Antibodies

In immunoblot analysis for Fhod3, affinity-purified rabbit polyclonal antibodies specific for Fhod3 were raised to the peptide of amino acid residues 873–974 and prepared as previously described (Kanaya et al., 2005; Taniguchi et al., 2009). In immunostaining for Fhod3 of sections of embryonic hearts (supplementary material Fig. S2), another anti-Fhod3 antibodies (anti-Fhod3-(C-20) antibodies), which were raised to the peptide of amino acid residues 1,567–1,586, were used (Kanaya et al., 2005; Kan-o et al., 2012). The mouse monoclonal antibody against α-actinin (clone EA-53) was purchased from Sigma-Aldrich; the mouse monoclonal antibody against glyceraldehyhyde-3-phosphate dehydrogenase (GAPDH) from Chemicon; and the fluorescent secondary antibody conjugated with Alexa Fluor 488 against mouse IgG from Invitrogen.

Analysis of embryonic heartbeat

Time-lapse recording of the embryonic heartbeat was performed according to the method of Nishii and Shibata (Nishii and Shibata, 2006) with minor modifications. Briefly, timed pregnant mice were deeply anesthetized by intraperitoneal injection of pentobarbital (50 mg/kg body weight) and dissected on a thermal plate at 37℃. For maintenance of the placental circulation, each decidual swelling was removed just before the observation. The embryos were dissected and their heartbeat was observed at 37℃ in M2 medium (Fulton and Whittingham, 1978). Here the extraembryonic membrane of E9.5–10.5 embryos was removed, while that of E8.5 embryos was intact. Images were recorded by a digital camera (DP21; Olympus) connected to a dissecting microscope (SZX16; Olympus). Kymographs were generated from time-lapse images in ImageJ software (National Institute of Health) by cropping a 2-pixel-wide rectangular region, making a montage of time-lapse sequences of cropped regions, and adjusting contrast.

Transmission electron microscopic analysis

Transmission electron microscopy of thin sections was performed as described by Koga et al. with minor modifications (Koga et al., 1990). Briefly, embryos were dissected and fixed with a fix buffer (2.5% glutaraldehyde, 0.1 M sucrose, 3 mM $CaCl_2$, and 0.1 M sodium cacodylate, pH 7.4) for 2 h, followed by rinse overnight at 4℃ in 0.1 M sodium cacodylate. Then embryos were postfixed for 1 hr with 1% OsO_4, dehydrated in ethanol and propylene oxide, and embedded in the Epon 812 resin. Thin sections containing the heart were stained for 10 min with uranyl acetate, and for 15 min with lead acetate, and then examined with a JEM-2000EX (JOEL).

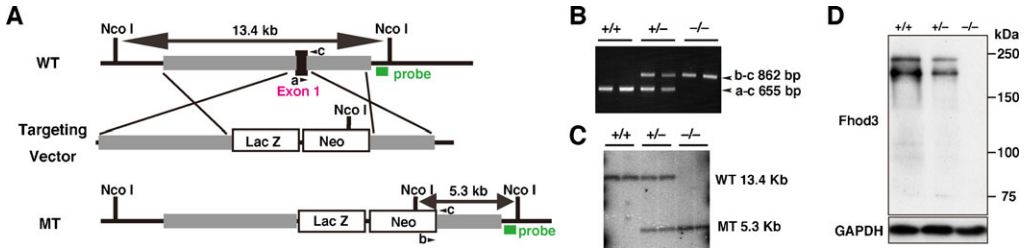

Fig. 1. Targeted disruption of the *Fhod3* gene. (**A**) Schematic representation of the Fhod3 gene-targeting strategy. Exon 1 of the *Fhod3* gene is represented as a box in black; flanking isogenic genomic DNAs in light gray; and the targeting cassette in white. Green bars indicate probes used for Southern blot analysis, and expected sizes of fragments obtained after NcoI digestion are indicated in base pair. Small black arrowheads indicate primers for PCR genotyping. (**B**) PCR analysis of the embryonic yolk sac DNAs from wild-type (+/+), $Fhod3^{+/-}$ (+/−), and $Fhod3^{-/-}$ (−/−) embryos. The 655-bp and 862-bp fragments were produced with the wild-type and recombinant alleles, respectively. (**C**) Southern blot analysis of NcoI-digested tail DNAs. The wild-type and recombinant alleles were detected as 13.4-kbp and 5.3-kbp fragments, respectively. (**D**) Detection of Fhod3 protein by immunoblot analysis. Proteins prepared from the whole embryo of wild-type (+/+), $Fhod3^{+/-}$ (+/−), and $Fhod3^{-/-}$ (−/−) mice at E9.5 were analyzed by immunoblot with anti-Fhod3 and anti-GAPDH antibodies.

TAC surgery and measurement of cardiac function

TAC surgery was performed on 8 to 10-wk-old male C57BL/6 mice as previously described (Nishida et al., 2008). Transthoracic echocardiography was performed using a Toshiba ultrasonic image analyzing system (Nemio-XG) equipped with 7.5 MHz imaging transducer. LV pressure and heart rate were measured with a micronanometer catheter (Millar 1.4F, SPR 671, Millar Instruments). Statistical comparisons were performed by two-way analysis of variance followed by the Bonferroni procedure for comparison of means.

Immunoblot analysis

Immunoblot analysis was performed as previously described (Kanaya et al., 2005; Taniguchi et al., 2009). Briefly, the whole body of E9.5 embryos was homogenized and sonicated at 4℃ in a lysis buffer (10% glycerol, 135 mM NaCl, 5 mM EDTA, and 20 mM Hepes, pH 7.4) containing Protease Inhibitor Cocktail (Sigma-Aldrich). The lysates were applied to SDS-PAGE and transferred to a polyvinylidene difluoride membrane (Millipore), which was probed with the anti-Fhod3 antibodies, followed by development using ECL-plus (GE Healthcare) for visualization of the antibodies. For estimation of the amount of Fhod3, densitometric analysis was performed using a LAS-1000 image analyzer (Fujifilm).

Results

Disruption of both *Fhod3* alleles leads to embryonic lethality by E11.5

To clarify the role of Fhod3 *in vivo*, we generated a targeted deletion of *Fhod3* exon 1 in embryonic stem cells by replacing it with *β-galactosidase* (*lacZ*) reporter gene (Fig. 1A). Adult heterozygous $Fhod3^{+/-}$ mice appeared phenotypically normal and fertile. However, intercrosses of $Fhod3^{+/-}$ mice did not produce any $Fhod3^{-/-}$ mice in their litters. PCR genotyping of yolk sac DNAs (Fig. 1B) revealed that $Fhod3^{-/-}$ embryos were present until E11.5, but not beyond that point (Table 1). Although the genotypes of embryos at E8.5–10.5 fit reasonably well to a Mendelian distribution, $Fhod3^{-/-}$ embryos were resorbed by E12.5. Southern blot analysis of genomic DNAs isolated from the whole body of embryos confirmed the genotype determined by PCR using yolk sac DNAs (Fig. 1C). As demonstrated by immunoblot analysis of the whole body extracts at E9.5, $Fhod3^{-/-}$ embryos had no detectable Fhod3 protein, whereas $Fhod3^{+/-}$ embryos had about 45.1±5.0% (n=4) of the amount of Fhod3 in wild-type embryos (Fig. 1D). Fhod3 was detected as doublet, where the upper and lower bands denote the cardiac and brain isoforms, respectively (supplementary material Fig. S1).

Table 1. Genotypes of offspring from heterozygous matings of $Fhod3^{+/-}$ mice.

Stage	$Fhod3^{+/+}$	$Fhod3^{+/-}$	$Fhod3^{-/-}$
E8.5	18	50	20
E9.5	39	91	38
E10.5	24 (1)	65 (1)	27 (1)
E11.5	31 (2)	44	9 (7)
E12.5	9	11	0 (3)
P7	83	160	0

Numbers in parenthesis represent those of resorbed embryos.

$Fhod3^{-/-}$ embryos are grossly stunted and malformed with aborted development of the myocardium at mid-gestation

We examined expression of the targeted $Fhod3^{lacZ}$ allele during embryogenesis by X-gal staining of heterozygous $Fhod3^{+/-}$ embryos, which were morphologically indistinguishable from wild-type embryos (Fig. 2A, upper and middle panels). X-gal staining was detected in the cardiac crescent of E7.5 embryos, and became prominent by E8.5. Weak X-gal staining was also detected in the neural tube at E8.5, becoming stronger at E9.5. Expression of Fhod3 in the heart and brain appears to be kept to adulthood, since Fhod3 is abundantly expressed in these tissues of adult mice (Kanaya et al., 2005). In addition, anti-Fhod3 (C-20) antibodies were able to detect endogenous Fhod3 protein at E11.5 and E13.5 (supplementary material Fig. S2). It should be noted that Fhod3 localizes as two closely spaced bands in middle of the sarcomere, as observed in embryonic hearts at later stages and adult ones (Kan-o et al., 2012) as well as in cultured cardiomyocytes (Iskratsch et al., 2010; Taniguchi et al., 2009).

$Fhod3^{-/-}$ embryos at E7.5–8.5 were comparable to wild-type and $Fhod3^{+/-}$ ones in size and gross morphology, appearing remarkably normal (Fig. 2A, lower panels). However, $Fhod3^{-/-}$ embryos died with a massive pericardial effusion and were resorbed by E12.5. At E9.5 they were smaller than their wild-type and $Fhod3^{+/-}$ littermates with obvious retardation in looping of the heart tube (Fig. 2A,B); and growth retardation was more evident at E10.5. As demonstrated by histological analysis of the ventricular wall of wild-type embryos (Fig. 2C, upper panels) and $Fhod3^{+/-}$ embryos (data not shown), myocardial mass increased by trabeculation at E9.5 and the increment became prominent at E10.5 (Sedmera et al., 2000). On the other hand, retardation or arrest of trabecula formation was observed at E10.5 in $Fhod3^{-/-}$ embryos: their myocardium appeared to lack well-defined trabeculae in comparison to that of the wild-type embryos (Fig. 2C, lower panels) as well as that of $Fhod3^{+/-}$ embryos (data not shown). Thus myocardial development is aborted by E10.5 in $Fhod3^{-/-}$ embryos; in contrast, the heart of $Fhod3^{+/-}$

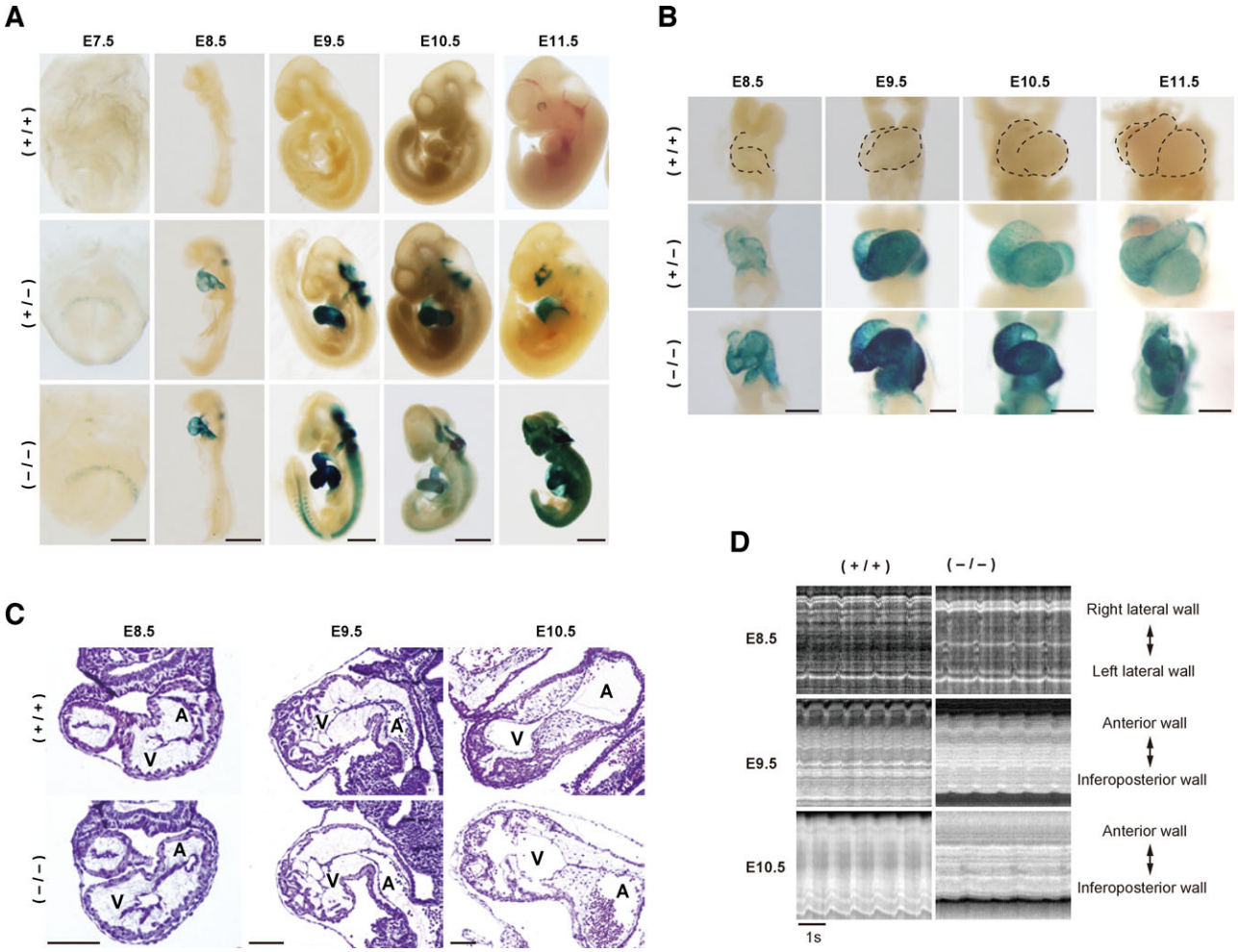

Fig. 2. Cardiac development in *Fhod3*$^{-/-}$ embryos at E9.5–11.5. (**A**) Whole-mount *lacZ* staining of *Fhod3*$^{+/+}$ (+/+), *Fhod3*$^{+/-}$ (+/−), and *Fhod3*$^{-/-}$ (−/−) embryos at E7.5–11.5. Bars: (E7.5) 250 µm; (E8.5/E9.5) 500 µm; (E10.5/E11.5) 1 mm. (**B**) Looping of the heart tube between E8.5 and E11.5 (front view). Bars: (E8.5/E9.5) 250 µm; (E10.5/E11.5) 500 µm. The contour of the wild-type heart is indicated by dotted lines. (**C**) Histological analysis of embryonic hearts between E8.5 and E10.5. Transverse sections (E8.5) and longitudinal sections (E9.5/E10.5) of hearts were stained with hematoxylin and eosin. Bars, 100 µm. (**D**) Kymographic analysis of beating of embryonic hearts between E8.5 and E10.5. The kymographs were generated from supplementary material Movies 1–6, and oriented so that the right lateral and left lateral walls are upward and downward, respectively (E8.5), or the anterior and inferoposterior walls are upward and downward, respectively (E9.5 and E10.5).

embryos is developed in the same manner as that of the wild-type ones, which is consistent with the finding that *Fhod3*$^{+/-}$ mice are grown up normally after birth and fertile. In addition, as expected, yolk sac vascular vessels were not well formed in *Fhod3*$^{-/-}$ mice (data not shown), a phenotype that is observed in other mutant mice that are defective in cardiomyogenesis (Huang et al., 2003; Krüger et al., 2000; Lucitti et al., 2007).

The heart of *Fhod3*$^{-/-}$ embryos beats spontaneously for a short period

To determine the effect of Fhod3 deficiency on embryonic heart function, we analyzed a contractive activity of *Fhod3*$^{-/-}$ and wild-type embryos. At E8.0–8.5, the heart of *Fhod3*$^{-/-}$ embryos did beat spontaneously, as that of wild-type ones (Fig. 2D, upper panels; supplementary material Movies 1, 2). At E9.5, the ventricular wall of the *Fhod3*$^{-/-}$ embryo heart was hypokinetic when compared with that of the wild-type heart (Fig. 2D, middle panels; supplementary material Movies 3, 4). At E10.5, a stage when a defect of trabeculation was evident in mutant embryos by histological analysis (Fig. 2C), the ventricle of *Fhod3*$^{-/-}$ embryos twitched only for the first 15–20 min after removal of the yolk sac, whereas the heart of wild-type embryos continued to beat vigorously during the observation period (15–20 min) (Fig. 2D, lower panels; supplementary material Movies 5, 6). Some of *Fhod3*$^{-/-}$ embryos at E10.5 had a massive pericardial effusion and their hearts did not beat at all (supplementary material Movie 7). Thus the heart of *Fhod3*$^{-/-}$ embryos initiates spontaneous contraction that continues only at initial stages of cardiac development. On the other hand, hearts of *Fhod3*$^{+/-}$ embryos functioned as those of the wild-type ones did (data not shown).

Premyofibrils fail to mature in the heart of *Fhod3*$^{-/-}$ embryos

To investigate the mechanism for impaired cardiac contraction in *Fhod3*$^{-/-}$ embryos, we examined myofibril assembly in the heart of *Fhod3*$^{-/-}$ embryos and wild-type ones by immunofluorescence staining for sarcomeric α-actinin, a protein that is a major component of both the I-Z-I complex and the Z-line and thus a suitable marker for myofibril assembly

(Fritz-Six et al., 2003; Holtzer et al., 1997). At E8.5, *Fhod3*$^{-/-}$ embryos were normal in morphology and histology (Fig. 2) and their hearts initiated spontaneous beating (supplementary material Movies 1, 2). At this stage, premyofibrils with Z-bodies, indicated by periodic dots of sarcomeric α-actinin, and with continuous or periodic F-actin staining were observed in *Fhod3*$^{-/-}$ embryos as well as wild-type ones (Fig. 3A). In wild-type embryos at E9.5, myofibrils contained regularly spaced bands of sarcomeric α-actinin with a striated F-actin staining pattern (Fig. 3B). Fully matured myofibrils, showing regular sarcomeric α-actinin striations (characteristic of mature Z-lines), were observed in wild-type embryos at E10.5 (Fig. 3C), when an increment of myocardial mass was obvious by histological analysis and the heart beat more vigorously (Fig. 2). Concomitantly, phalloidin staining became prominent by E10.5, indicating a marked increase in actin filaments. In contrast, no striated myofibrils was observed in the heart of *Fhod3*$^{-/-}$ embryos; instead a few numbers of premyofibril-like structures with irregularly spaced dots or aggregates of sarcomeric α-actinin were sparsely distributed (Fig. 3B,C). In addition, unlike wild-type embryos, intense staining with phalloidin was not observed in *Fhod3*$^{-/-}$ embryos. It is thus possible that, although premyofibrils with Z-bodies were formed in the E8.5 mutant embryos, they have been disassembled and/or aggregated by E9.5.

We further examined the ultrastructure of myofibrils using transmission electron microscopy (Fig. 3D; supplementary material Fig. S3). In the wild-type embryos, the sarcomere was well organized by E10.5 with mature Z-lines; and a part of the Z-lines associated with fascia adherens, which appears to be a forming intercalated disc. In contrast, in *Fhod3*$^{-/-}$ embryos, only irregular Z-body-like electron-dense spots were observed beneath the sarcolemma, *i.e.*, the plasma membrane of cardiomyocytes. Thus myofibrillogenesis in *Fhod3*$^{-/-}$ embryos appears to be aborted at the stage when premyofibrils mature into striated myofibrils.

Transgenic expression of wild-type Fhod3 in the heart rescues cardiac defects of *Fhod3*$^{-/-}$ embryos

In addition to high expression in the heart, Fhod3 was considerably expressed in the neural tube (Fig. 2A). All the *Fhod3*$^{-/-}$ embryos showed defects in neural tube closure, which is normally completed by E9.5 (Fig. 2A). This indicates that Fhod3 is involved in development of organs other than the heart. To investigate whether embryonic lethality of Fhod3 nulls at mid-gestation is caused by defects in the heart, we performed a transgenic rescue experiment by expressing Fhod3 specifically in the myocardium under the control of the α-myosin heavy chain (MHC) promoter. The well-characterized α-MHC promoter is specifically and highly expressed in the developing myocardium (Gulick et al., 1991; Kan-o et al., 2012). Hemizygous *Fhod3*$^{Tg(\alpha\text{-MHC-Fhod3})}$ mice survived to adulthood and were fertile without obvious abnormality. Although intercrosses of *Fhod3*$^{+/-}$ and *Fhod3*$^{+/-Tg(\alpha\text{-MHC-Fhod3})}$ did not produce any *Fhod3*$^{-/-Tg(\alpha\text{-MHC-Fhod3})}$ mice, analysis of embryos revealed that *Fhod3*$^{-/-Tg(\alpha\text{-MHC-Fhod3})}$ embryos developed well beyond the *Fhod3*$^{-/-}$ lethal stage (Table 2). As shown in Fig. 4A, the myocardium of the ventricle of *Fhod3*$^{-/-Tg(\alpha\text{-MHC-Fhod3})}$ embryos at E11.5 well developed with fine trabeculation, similarly to that of wild-type embryos. At E17.5, *Fhod3*$^{-/-Tg(\alpha\text{-MHC-Fhod3})}$ embryos, having a well-developed heart,

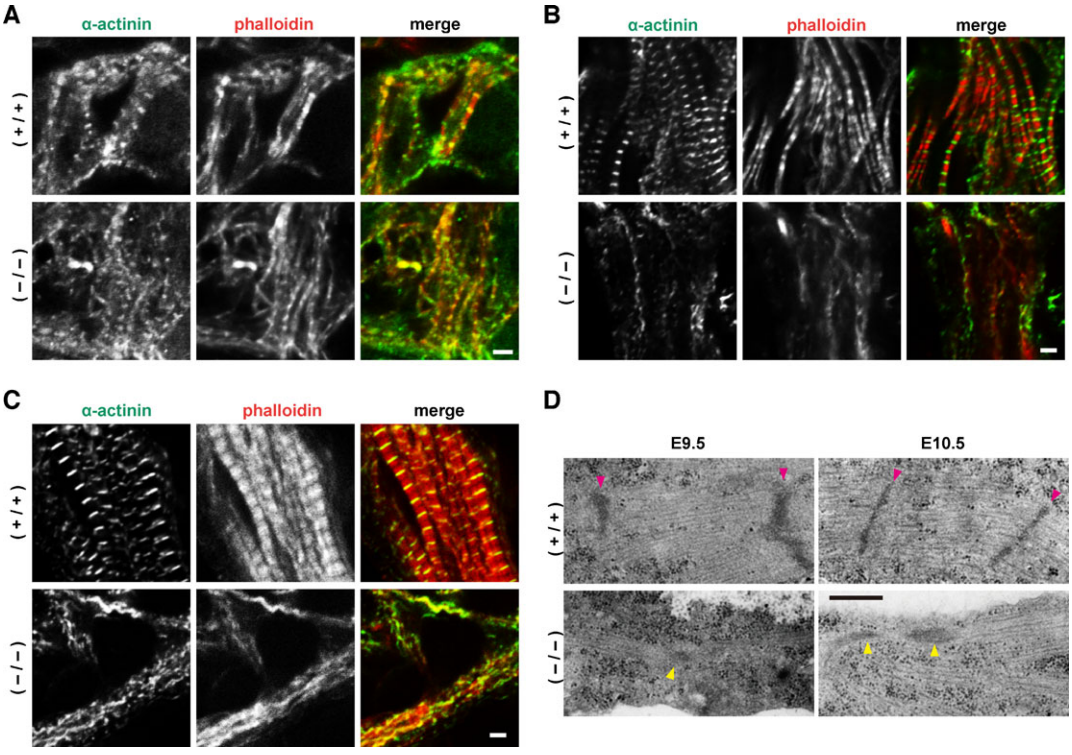

Fig. 3. Myofibrils in the embryonic heart. (**A–C**) Confocal fluorescence micrographs of hearts of wild-type (+/+) and *Fhod3*$^{-/-}$ (−/−) embryos. Sections of embryonic hearts at E 8.5 (A), E9.5 (B), and E10.5 (C) were subjected to immunofluorescent staining for α-actinin (green) and phalloidin staining for F-actin (red). Bars, 2 µm. (**D**) Electron micrographs of thin sections of wild-type (+/+) and *Fhod3*$^{-/-}$ (−/−) hearts at E9.5 and E10.5. Magenta and yellow arrowheads indicate Z-lines and Z-body-like electron-dense spots, respectively. Bar, 500 nm.

Table 2. Genotypes of offspring from matings of *Fhod3*$^{+/-}$ × *Fhod3*$^{+/-\text{Tg(α-MHC-Fhod3)}}$.

Stage	*Fhod3*$^{+/+}$	*Fhod3*$^{+/+}$;*Tg*$^{+}$	*Fhod3*$^{+/-}$	*Fhod3*$^{+/-}$;*Tg*$^{+}$	*Fhod3*$^{-/-}$	*Fhod3*$^{-/-}$;*Tg*$^{+}$
E10.5	1	4	4	5	2	1
E11.5	2	1	3	1	0	2
E12.5	3	1	4	6	0	2
E16.5	1	1	10	7	0	2
E17.5	5	7	4	8	0	5

were indistinguishable from wild-type embryos at the morphological level except for exencephaly (Fig. 4B). In the heart of *Fhod3*$^{-/-\text{Tg(α-MHC-Fhod3)}}$ embryos, myofibrils exhibited regularly spaced bands of sarcomeric α-actinin along with a striated F-actin pattern at E10.0 (Fig. 4C), and fully matured myofibrils were found at E17.5 (Fig. 4D); full maturation was indicated by clear gaps in F-actin staining at the center of the sarcomere (Fig. 4D). Thus transgenic expression of Fhod3 in the heart sufficiently rescues defects in sarcomere organization and myocardial development, indicating that the lethality of *Fhod3*$^{-/-}$ mice by E11.5 occurs as the direct result from aborted cardiac development.

Overexpression of an actin binding-defective Fhod3 in the heart inhibits myofibril maturation

To investigate how Fhod3 functions in heart development, we generated transgenic mice expressing a mutant Fhod3 carrying the I1127A substitution under the control of the α-MHC promoter (*Fhod3*$^{\text{Tg(α-MHC-Fhod3IA)}}$) (supplementary material Fig. S4). The mutant protein, defective in binding to actin, fails to induce actin assembly in HeLa cells and to promote sarcomere organization in cultured cardiomyocytes (Taniguchi et al., 2009). Hemizygous *Fhod3*$^{\text{Tg(α-MHC-Fhod3IA)}}$ mice survived to adulthood and were fertile. On the other hand, their intercrosses with *Fhod3*$^{+/-}$ mice failed to generate the expected Mendelian ratio (25%) of inheritance in offspring: *Fhod3*$^{+/-\text{Tg(α-MHC-Fhod3IA)}}$ made up only 14.4% of all pups (14 of 97 pups) at postnatal day 8 (P8) (Fig. 5A). These *Fhod3*$^{+/-\text{Tg(α-MHC-Fhod3IA)}}$ pups all died within 3 weeks after birth. Since the activity of the α-MHC promoter is enhanced after birth (Gulick et al., 1991), *Fhod3*$^{+/-\text{Tg(α-MHC-Fhod3IA)}}$ neonates, with an increased amount of Fhod3 (I1127A), may be affected more severely than the corresponding embryos. The heart of *Fhod3*$^{+/-\text{Tg(α-MHC-Fhod3IA)}}$ at P7 was markedly dilated and its ventricular wall was thinner with the lack of the non-compacted layer of the myocardium, compared with the heart of *Fhod3*$^{+/-}$ mice at P7 (Fig. 5B). In the mutant heart there existed myofibrils with various degrees of maturation defect, such as ones containing continuous F-actin and α-actinin aggregates concentrated along the sarcolemma (Fig. 5C). In contrast to *Fhod3*$^{+/-\text{Tg(α-MHC-Fhod3IA)}}$ mice, *Fhod3*$^{+/-}$ mice without the transgene were functionally equivalent to wild-type ones even after pressure overload by surgical transverse aortic constriction (TAC) (Fig. 5D; supplementary material Fig. S5). These findings suggest that cardiac overexpression of a mutant Fhod3 protein, defective in an *in vivo* actin-assembling activity, inhibits myofibril maturation, leading to compromised heart function. Thus the actin-assembling activity appears to be crucial for Fhod3 function during cardiac development.

Discussion

In the present study we show that the mammalian formin Fhod3 plays a crucial role in sarcomere (and myofibril) maturation

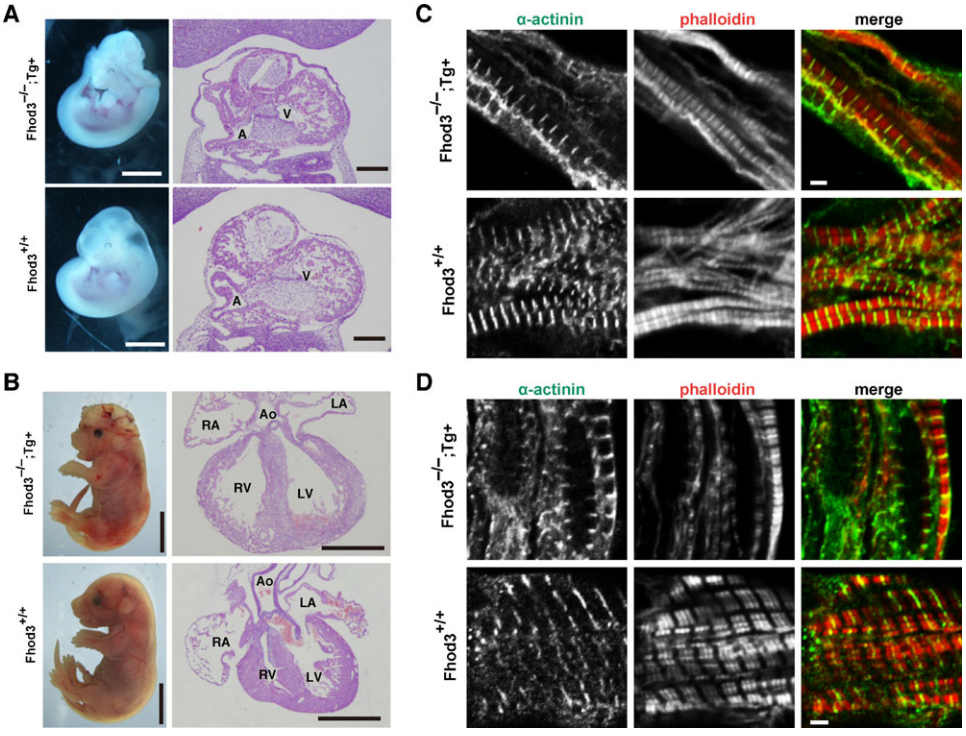

Fig. 4. Effect of transgenic expression of Fhod3 in the heart of *Fhod3*$^{-/-}$ mice. (**A**,**B**) Whole-mount (left panels) and histological (right panels) analyses of wild-type (*Fhod3*$^{+/+}$) and *Fhod3*$^{-/-\text{Tg(α-MHC-Fhod3)}}$ (*Fhod3*$^{-/-}$;*Tg*$^{+}$) embryos at E11.5 (A) and E17.5 (B). V, ventricle; A, atrium; LV, left ventricle; RV, right ventricle; LA, left atrium; RA, right atrium; Ao, aorta. Bars in A: (left) 1 mm; (right) 200 µm. Bars in B: (left) 5 mm; (right) 1 mm. (**C**,**D**) Confocal fluorescence micrographs of hearts of wild-type (+/+) and *Fhod3*$^{-/-\text{Tg(α-MHC-Fhod3)}}$ (*Fhod3*$^{-/-}$;*Tg*$^{+}$) embryos at E10.0 (C) and E17.5 (D). Sections of embryonic hearts were subjected to immunofluorescent staining for α-actinin (green) and phalloidin staining for F-actin (red). Bars, 2 µm.

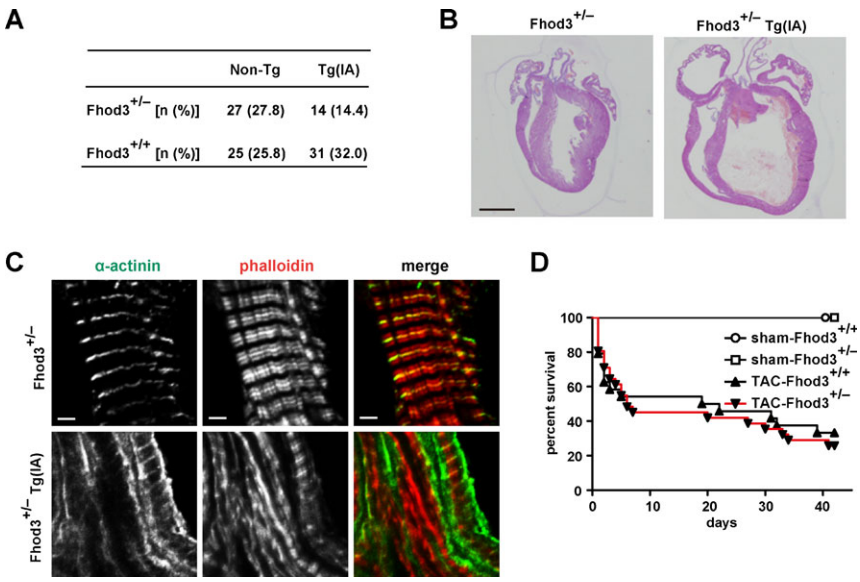

Fig. 5. Transgenic expression of Fhod3 (I1127A) in the heart. (**A**) Genotypes of offspring from the mating of $Fhod3^{+/-}$ × $Fhod3^{+/+Tg(\alpha\text{-MHC-Fhod31A})}$. The number in parentheses indicates the percentage of the total number of offspring. (**B**) Histological analysis of hearts from $Fhod3^{+/-}$ and $Fhod3^{+/-Tg(\alpha\text{-MHC-Fhod31A})}$ ($Fhod3^{+/-}$Tg(IA)) mice at age of 8 day. Bars, 100 µm. (**C**) Confocal fluorescence micrographs of hearts from $Fhod3^{+/-}$ and $Fhod3^{+/-Tg(\alpha\text{-MHC-Fhod31A})}$ ($Fhod3^{+/-}$Tg(IA)) mice at P8. Sections of hearts were subjected to immunofluorescent staining for α-actinin (green) and phalloidin staining for F-actin (red). Bars, 2 µm. (**D**) Kaplan-Meier survival curves versus days after TAC. TAC-$Fhod3^{+/+}$ (n=24); TAC-$Fhod3^{+/-}$ (n=31); sham-$Fhod3^{+/+}$ (n=4); and sham-$Fhod3^{+/-}$ (n=4) mice.

during heart development. $Fhod3^{-/-}$ mice are embryonic lethal with a massive pericardial effusion. Although the developing heart tube of $Fhod3^{-/-}$ embryos initiates rightward looping, subsequent chamber formation and myocardial development with trabeculation are aborted. The present histochemical analysis demonstrates that premyofibrils with periodic dots of α-actinin are formed by E8.5 in the heart, but fail to mature into striated mature myofibrils. These phenotypes are similar to those of conventional knock-out mice of Tmod1 (Fritz-Six et al., 2003). In Tmod1-null embryos, although myofibril maturation does not occur, F-actin content apparently increases beyond E8.5 (Fritz-Six et al., 2003). In contrast, the increase is not observed in Fhod3-null embryos, supporting the idea that Fhod3 is involved in actin assembly *per se* during myofibril maturation.

Transgenic expression of Tmod1 in the heart using α-MHC promoter completely rescues the viability of Tmod1-null mice (McKeown et al., 2008). On the other hand, heart-specific expression of Fhod3 under the control of the same promoter allows $Fhod3^{-/-}$ embryos to develop until before birth, but fails to restore exencephaly. The cardiac defects thus do not appear to be responsible for failure in neural tube closure, which may be attributed to the absence of Fhod3 in the brain. On the other hand, the *in vivo* cardiac defects agree well with the observation that sarcomere organization is disrupted by depletion of Fhod3 in cultured cardiomyocytes (Iskratsch et al., 2010; Taniguchi et al., 2009).

Spontaneous contraction of the developing heart initiates at the stage when it consists of a thin layer of the myocardium composed of immature cardiomyocytes containing premyofibrils. Fhod3 does not seem to play a major role at this stage, because the heart tube with premyofibrils formed does beat spontaneously in $Fhod3^{-/-}$ embryos. On the other hand, cardiac premyofibrils fail to mature into striated myofibrils in the absence of Fhod3. The maturation is known to require a drastic increase in well-aligned actin filaments, which is induced by facilitated actin polymerization (Ono, 2010). Consistent with this, myofibril maturation is disturbed by depletion of actin nucleators such as leiomodin and nebulin (in conjunction with N-WASP) from striated muscle cells (Chereau et al., 2008; McElhinny et al., 2005; Takano et al., 2010). The marked increment in actin filaments is not observed in $Fhod3^{-/-}$ embryos, suggesting that Fhod3 contributes to regulation of actin dynamics during myofibril maturation. This is supported by the previous *in vitro* finding that expression of wild-type Fhod3, but not a mutant Fhod3 defective in an actin-assembling activity, rescues sarcomere organization in cardiomyocytes depleted of endogenous Fhod3 (Taniguchi et al., 2009).

We have recently demonstrated that, in both embryonic (at around E16) and adult hearts, Fhod3 localizes in the middle of the sarcomere (Kan-o et al., 2012); the same localization of Fhod3 is observed in the embryonic heart at earlier stages (E11.5 and E13.5) (supplementary material Fig. S2). In more detail, Fhod3 localizes not at the pointed ends of thin actin filaments but to a more peripheral zone, where thin filaments overlap with thick myosin filaments (Kan-o et al., 2012). At the overlapping region, localized mechanical breakage of actin filaments may occur during muscle contraction, presumably due to myosin-driven force (Murphy et al., 1988). The breakage may subsequently induce reorganization of actin filaments at the overlapping region; it has been suggested that acto-myosin contraction causes actin filament disassembly and reorganization in muscle cells as well as non-muscle cells (Skwarek-Maruszewska et al., 2009; Wilson et al., 2010). The contraction-dependent reorganization of actin filaments may be possibly involved in Fhod3-mediated myofibril maturation during heart development. Further studies are needed to elucidate the precise molecular mechanism of Fhod3 action in cardiogenesis.

It has recently been reported that Daam1, another member of the formin family proteins, is required for heart morphogenesis (Li et al., 2011). The onset of cardiac expression of Daam1 is later than that of Fhod3; Fhod3 expression can be detected in the cardiac crescent of E7.5 embryos (Fig. 2A). In addition, cardiac defects induced by Daam1 depletion in mice become evident only after myofibril maturation, leading to embryonic lethality after E14.5. In contrast, Fhod3-deficient mice exhibit lethality by E11.5, as shown in the present study. Thus Daam1 seems to participate in a later stage of cardiac development, which may regulate cardiomyocyte adhesion or migration (Li et al., 2011). Cardiac development likely requires multiple members of formin family proteins to regulate actin cytoskeleton at different stages.

As shown in the present study, overexpression of a mutant Fhod3 protein with the I1127A substitution, defective in an *in vivo* actin-assembling activity (Taniguchi et al., 2009), can induce cardiomyopathic changes with immature myofibrils even in the presence of a wild-type allele. Since formin family proteins are known to function as a dimer (Goode and Eck, 2007; Pollard, 2007), such a mutant Fhod3 protein may form a non-functional heterodimer with the wild-type protein, raising the possibility that a loss-of-function mutation in the FHOD3 gene may cause familial cardiomyopathy with autosomal dominant inheritance.

Acknowledgements

We thank Drs. Masaya Oki (Kyushu University), Yuichi Shima (Kyushu University), and Kanako Miyabayashi (Kyushu University) for advice on analysis of embryonic mice; Dr. Kiyomasa Nishii (National Defense Medical College) for advice on observation of heartbeat using videomicroscopy; Dr. Jeffery Robbins (Cincinnati Children's Hospital Medical Center) for providing α-MHC promoter; Masato Tanaka (Kyushu University) for generation of transgenic mice; Masafumi Sasaki (Kyushu University) and Ryo Ugawa (Kyushu University) for electron microscopic analysis; Norihiko Kinoshita (Kyushu University) for histochemical analysis; Yohko Kage (Kyushu University), Natsuko Morinaga (Kyushu University), and Namiko Kubo (Kyushu University) for technical assistance; and Minako Nishino (Kyushu University) for secretarial assistance. We also appreciate, for technical support, the Research Support Center, Kyushu University Graduate School of Medical Sciences and the Laboratory for Technical Support, Medical Institute of Bioregulation, Kyushu University. This work was supported in part by Grants-in-Aid for Scientific Research and Targeted Proteins Research Program (TPRP) from the Ministry of Education, Culture, Sports, Science and Technology (MEXT), Japan, and by the Japan Foundation for Applied Enzymology and the Nakatomi Foundation.

Competing Interests

The authors have no competing interests to declare.

References

Chereau, D., Boczkowska, M., Skwarek-Maruszewska, A., Fujiwara, I., Hayes, D. B., Rebowski, G., Lappalainen, P., Pollard, T. D. and Dominguez, R. (2008). Leiomodin is an actin filament nucleator in muscle cells. *Science* **320**, 239-243.

Chesarone, M. A., DuPage, A. G. and Goode, B. L. (2010). Unleashing formins to remodel the actin and microtubule cytoskeletons. *Nat. Rev. Mol. Cell Biol.* **11**, 62-74.

Clark, K. A., McElhinny, A. S., Beckerle, M. C. and Gregorio, C. C. (2002). Striated muscle cytoarchitecture: an intricate web of form and function. *Annu. Rev. Cell Dev. Biol.* **18**, 637-706.

Fritz-Six, K. L., Cox, P. R., Fischer, R. S., Xu, B., Gregorio, C. C., Zoghbi, H. Y. and Fowler, V. M. (2003). Aberrant myofibril assembly in tropomodulin1 null mice leads to aborted heart development and embryonic lethality. *J. Cell Biol.* **163**, 1033-1044.

Fulton, B. P. and Whittingham, D. G. (1978). Activation of mammalian oocytes by intracellular injection of calcium. *Nature* **273**, 149-151.

Goode, B. L. and Eck, M. J. (2007). Mechanism and function of formins in the control of actin assembly. *Annu. Rev. Biochem.* **76**, 593-627.

Gregorio, C. C. and Antin, P. B. (2000). To the heart of myofibril assembly. *Trends Cell Biol.* **10**, 355-362.

Gulick, J., Subramaniam, A., Neumann, J. and Robbins, J. (1991). Isolation and characterization of the mouse cardiac myosin heavy chain genes. *J. Biol. Chem.* **266**, 9180-9185.

Holtzer, H., Hijikata, T., Lin, Z. X., Zhang, Z. Q., Holtzer, S., Protasi, F., Franzini-Armstrong, C. and Sweeney, H. L. (1997). Independent assembly of 1.6 μm long bipolar MHC filaments and I-Z-I bodies. *Cell Struct. Funct.* **22**, 83-93.

Huang, C., Sheikh, F., Hollander, M., Cai, C., Becker, D., Chu, P. H., Evans, S. and Chen, J. (2003). Embryonic atrial function is essential for mouse embryogenesis, cardiac morphogenesis and angiogenesis. *Development* **130**, 6111-6119.

Iskratsch, T., Lange, S., Dwyer, J., Kho, A. L., dos Remedios, C. and Ehler, E. (2010). Formin follows function: a muscle-specific isoform of FHOD3 is regulated by CK2 phosphorylation and promotes myofibril maintenance. *J. Cell Biol.* **191**, 1159-1172.

Kanaya, H., Takeya, R., Takeuchi, K., Watanabe, N., Jing, N. and Sumimoto, H. (2005). Fhos2, a novel formin-related actin-organizing protein, probably associates with the nestin intermediate filament. *Genes Cells* **10**, 665-678.

Kan-o, M., Takeya, R., Taniguchi, K., Tanoue, Y., Tominaga, R. and Sumimoto, H. (2012). Expression and subcellular localization of mammalian formin Fhod3 in the embryonic and adult heart. *PLoS ONE* **7**, e34765.

Koga, Y., Sasaki, M., Nakamura, K., Kimura, G. and Nomoto, K. (1990). Intracellular distribution of the envelope glycoprotein of human immunodeficiency virus and its role in the production of cytopathic effect in $CD4^+$ and $CD4^-$ human cell lines. *J. Virol.* **64**, 4661-4671.

Krüger, O., Plum, A., Kim, J. S., Winterhager, E., Maxeiner, S., Hallas, G., Kirchhoff, S., Traub, O., Lamers, W. H. and Willecke, K. (2000). Defective vascular development in connexin 45-deficient mice. *Development* **127**, 4179-4193.

Kulandavelu, S., Qu, D., Sunn, N., Mu, J., Rennie, M. Y., Whiteley, K. J., Walls, J. R., Bock, N. A., Sun, J. C., Covelli, A. et al. (2006). Embryonic and neonatal phenotyping of genetically engineered mice. *ILAR J.* **47**, 103-117.

Li, D., Hallett, M. A., Zhu, W., Rubart, M., Liu, Y., Yang, Z., Chen, H., Haneline, L. S., Chan, R. J., Schwartz, R. J. et al. (2011). Dishevelled-associated activator of morphogenesis 1 (Daam1) is required for heart morphogenesis. *Development* **138**, 303-315.

Littlefield, R. S. and Fowler, V. M. (2008). Thin filament length regulation in striated muscle sarcomeres: pointed-end dynamics go beyond a nebulin ruler. *Semin. Cell Dev. Biol.* **19**, 511-519.

Liu, R., Linardopoulou, E. V., Osborn, G. E. and Parkhurst, S. M. (2010). Formins in development: orchestrating body plan origami. *Biochim. Biophys. Acta* **1803**, 207-225.

Lucitti, J. L., Jones, E. A., Huang, C., Chen, J., Fraser, S. E. and Dickinson, M. E. (2007). Vascular remodeling of the mouse yolk sac requires hemodynamic force. *Development* **134**, 3317-3326.

McElhinny, A. S., Schwach, C., Valichnac, M., Mount-Patrick, S. and Gregorio, C. C. (2005). Nebulin regulates the assembly and lengths of the thin filaments in striated muscle. *J. Cell Biol.* **170**, 947-957.

McKeown, C. R., Nowak, R. B., Moyer, J., Sussman, M. A. and Fowler, V. M. (2008). Tropomodulin1 is required in the heart but not the yolk sac for mouse embryonic development. *Circ. Res.* **103**, 1241-1248.

Moorman, A. F. and Christoffels, V. M. (2003). Cardiac chamber formation: development, genes, and evolution. *Physiol. Rev.* **83**, 1223-1267.

Murphy, D. B., Gray, R. O., Grasser, W. A. and Pollard, T. D. (1988). Direct demonstration of actin filament annealing *in vitro*. *J. Cell Biol.* **106**, 1947-1954.

Nishida, M., Sato, Y., Uemura, A., Narita, Y., Tozaki-Saitoh, H., Nakaya, M., Ide, T., Suzuki, K., Inoue, K., Nagao, T. et al. (2008). $P2Y_6$ receptor-$G\alpha_{12/13}$ signalling in cardiomyocytes triggers pressure overload-induced cardiac fibrosis. *EMBO J.* **27**, 3104-3115.

Nishii, K. and Shibata, Y. (2006). Mode and determination of the initial contraction stage in the mouse embryo heart. *Anat. Embryol. (Berl.)* **211**, 95-100.

Ono, S. (2010). Dynamic regulation of sarcomeric actin filaments in striated muscle. *Cytoskeleton* **67**, 677-692.

Paul, A. S. and Pollard, T. D. (2009). Review of the mechanism of processive actin filament elongation by formins. *Cell Motil. Cytoskeleton* **66**, 606-617.

Pollard, T. D. (2007). Regulation of actin filament assembly by Arp2/3 complex and formins. *Annu. Rev. Biophys. Biomol. Struct.* **36**, 451-477.

Sanger, J. W., Kang, S., Siebrands, C. C., Freeman, N., Du, A., Wang, J., Stout, A. L. and Sanger, J. M. (2005). How to build a myofibril. *J. Muscle Res. Cell Motil.* **26**, 343-354.

Sedmera, D., Pexieder, T., Vuillemin, M., Thompson, R. P. and Anderson, R. H. (2000). Developmental patterning of the myocardium. *Anat. Rec.* **258**, 319-337.

Shima, Y., Zubair, M., Ishihara, S., Shinohara, Y., Oka, S., Kimura, S., Okamoto, S., Minokoshi, Y., Suita, S. and Morohashi, K. (2005). Ventromedial hypothalamic nucleus-specific enhancer of Ad4BP/SF-1 gene. *Mol. Endocrinol.* **19**, 2812-2823.

Skwarek-Maruszewska, A., Hotulainen, P., Mattila, P. K. and Lappalainen, P. (2009). Contractility-dependent actin dynamics in cardiomyocyte sarcomeres. *J. Cell Sci.* **122**, 2119-2126.

Taber, L. A. (1998). Mechanical aspects of cardiac development. *Prog. Biophys. Mol. Biol.* **69**, 237-255.

Takano, K., Watanabe-Takano, H., Suetsugu, S., Kurita, S., Tsujita, K., Kimura, S., Karatsu, T., Takenawa, T. and Endo, T. (2010). Nebulin and N-WASP cooperate to cause IGF-1-induced sarcomeric actin filament formation. *Science* **330**, 1536-1540.

Taniguchi, K., Takeya, R., Suetsugu, S., Kan-o, M., Narusawa, M., Shiose, A., Tominaga, R. and Sumimoto, H. (2009). Mammalian formin fhod3 regulates actin assembly and sarcomere organization in striated muscles. *J. Biol. Chem.* **284**, 29873-29881.

Wilson, C. A., Tsuchida, M. A., Allen, G. M., Barnhart, E. L., Applegate, K. T., Yam, P. T., Ji, L., Keren, K., Danuser, G. and Theriot, J. A. (2010). Myosin II contributes to cell-scale actin network treadmilling through network disassembly. *Nature* **465**, 373-377.

Yagi, T., Tokunaga, T., Furuta, Y., Nada, S., Yoshida, M., Tsukada, T., Saga, Y., Takeda, N., Ikawa, Y. and Aizawa, S. (1993). A novel ES cell line, TT2, with high germline-differentiating potency. *Anal. Biochem.* **214**, 70-76.